K-BAND BARITT DOPPLER DETECTORS*

J. R. East, P. J. McCleer and G. I. Haddad
Electron Physics Laboratory
Department of Electrical and Computer Engineering
The University of Michigan
Ann Arbor, MI 48109

Abstract

The properties of K-band BARITT devices for use as self-mixing doppler detectors have been studied experimentally and with a simplified computer model. The computer results predict sensitive BARITT doppler operation even at low power levels. The experimental results show that the BARITT is superior to both IMPATT and Gunn devices for use as self-oscillating doppler detectors in this frequency range.

Introduction

Previous work at X-band has shown that the BARITT is superior to both the IMPATT and Gunn devices as a self-oscillating detector, requiring lower dc power, lower microwave power and having better path loss and minimum detectable signal characteristics.[1] This paper will discuss the reasons for these advantages, based on a simplified computer analysis of the BARITT, and will present further experimental data on three devices operating in the K-band frequency range.

Computer Model and Results

A simplified, analytical, intermediate-amplitude model for a BARITT diode oscillator has been developed to help in the understanding of the detector measurements. The model assumes (a) carrier injection over a forward-biased junction and (b) a carrier delay region (the reverse-biased junction) that is divided into two subregions of pure diffusion and pure drift, respectively. Previous theoretical treatment of negative-resistance diode doppler detectors[2,3] has shown that for orthogonal tuning the amplitude of the detected doppler voltage is proportional to $[(\partial V_{dc}/\partial V_{RF})|Z_D/(\partial Z_D/\partial V_{RF})|]|_{V_o}$, where V_{dc} is the dc bias voltage across the diode, V_{RF} is the magnitude of the oscillator RF voltage, V_o is the magnitude of the RF voltage without the doppler signal present, and Z_D is the complex diode impedance. To solve for these quantities using the simplified analysis, a single component RF voltage is specified to exist across the forward-biased region of the diode. When exponential current flow and an average value for the forward-biased depletion-region width are assumed, the impedance of the forward-biased region can be expressed as the parallel combination of the linear depletion layer capacitive reactance and the highly nonlinear exponential diode resistance. A similar formulation using the modified Bessel function expansion for the exponentially injected current was presented by several investigators.[4,5] When the injection point modulation is neglected, the remaining active region of the diode is divided into linear impedance lengths of exclusive diffusion or drift current flow. The region of pure diffusion is intended to simulate the current flow and delay in the low-field region of the diode immediately adjacent to the injection point. The region of pure drift gives rise to the main delay mechanism of the diode and is comparable to the saturated drift region of an IMPATT diode. Computational experience has indicated that the optimum length for the region of pure diffusion is one half the distance that the electric field needs to rise to a value that would give saturated drift, 3×10^5 V/cm for holes in Si. Higher-order approximations, i.e., a number of low-field delay regions with combined diffusion and drift were studied for the small-signal case but it was found that sufficient detail and insight could be attained with the simpler two-length formulation. The impedances of the two delay regions are determined by matching forward-wave components of voltage and current at the appropriate boundaries. The ratio of voltage across each region to the total diode current can then be solved for as well as the total voltage across the entire diode. The large-signal rectification effect is given by the expansion of the injected current into its dc and ac components.

Table 1 gives the parameters of the two diode structures studied theoretically and the approximate parameters of the device used in the experimental measurements. For a BARITT diode oscillator, in general, the optimum frequency of operation is determined by the active base length and the power capability is determined by its doping. Thus Device B is capable of higher power even though it is operating at a higher frequency. The doping levels in both devices are below the allowable maximum set by the onset of impact ionization in the high-field region. Figure 1 is an R-X plot at 23 GHz for Device B with the dc current density J_o and the RF drive level V_{RF} as parameters. As can be seen, the relative change in the value of the total diode impedance is quite small over the entire range of parameters shown. A 1-percent change radius for a fixed operating point (M), $J_o = 400$ A/cm^2, $V_{RF} = 6.6$ V, is shown by the shaded area. The rectification effect between V_{dc} and V_{RF} for Device B at 23 GHz is shown in Fig. 2. Note that the effect, a decrease in V_{dc} with V_{RF}, is evident even for small values of RF drive. This is to be compared with the operation of an IMPATT diode oscillator where the rectification effect is not noticeable until relatively large RF drives are encountered. The external circuit sets the lower limit on the value of RF load resistance that can be presented to the diode. Thus a power-tuning procedure can be envisioned as follows: The circuit is tuned to present its lowest value of resistance and the needed reactance at the optimum bias and operating frequency of the diode. The bias current is then lowered while leaving the circuit tuning untouched, reducing the output RF power and changing the oscillating frequency slightly. From the R-X plot of Fig. 1 it is obvious that changing the dc bias current while requiring the real part of the impedance to remain constant would require only a minute change in circuit reactance to maintain a constant operating frequency. Conversely, leaving the circuit reactance constant will produce only minute changes in oscillating frequency. The physical reason for this behavior is that the diode

*Research partially sponsored by the Air Force Office of Scientific Research, Air Force Systems Command, USAF, under Grant No. AFOSR-76-2939A and by the U. S. Army Research Office under Contract No. DAAG29-76-G-0232.

is a punched-through structure and is dominated by its cold capacitance. The preceding discussion leads to the choice of a constant load resistance power tuning curve at a constant frequency as the basis for comparing detection sensitivities for various levels of operation of the same device. Such a tuning curve is shown in Fig. 2 for an assumed $R_L = 2 \times 10^{-5}$ Ω-cm^2 normalized to the junction area of the diode.

Finally, the computed detected doppler voltage, normalized to path loss, is shown in Fig. 3 for both diode structures studied. Note that the doppler voltage decreases with RF power but not nearly at the same rate. For example, between operating points (P) and (Q) of Device B, the RF output power changes by 23.6 dB but the detected doppler signal decreases by only 9.7 dB. Thus, assuming that the diode noise-to-carrier ratio is constant with changes in bias,[6] the diode is actually a more sensitive receiver in terms of minimum detectable signal (MDS) when operated at lower power. This phenomenon has been observed at X-band[1] as well as in the present study.

Experimental Results

The doppler sensitivity of the Gunn, IMPATT and BARITT devices was measured using the circuit shown in Fig. 4. The operation of the circuit can be explained using the phasor diagram in Fig. 5. The phasor of the doppler signal rotates around the tip of the RF voltage phasor. It has a magnitude kV_{RF} equal to the magnitude of the RF voltage reduced by the path loss k. The angular frequency is $2\pi f_d$. The length of the total RF voltage $V_{RF} + kV_{RF}$ is to first order $V_{RF} + kV_{RF} \cos \omega_d t$, and the change in magnitude of total RF voltage results in a modulation of the dc bias voltage through the $\partial V_{dc}/\partial V_{RF}$ term discussed previously. The experimental circuit replaces the $kV_{RF} \sin \omega_d t$ term by a term $\pm kV_{RF}$ which is square-wave switched at the doppler frequency. The resulting change in dc voltage is separated from the bias voltage by a dc blocking capacitor and is displayed using a wave analyzer.

Experimental results for a BARITT detector operating at approximately 25 V and 21.3 GHz are shown in Fig. 6. This figure shows characteristics that are similar to BARITT operation at X-band[1] as well as other K-band BARITT devices tested. First, the BARITT is able to operate with small prime and microwave power levels. The prime power level for this device varies between 75 and 225 mW and the microwave power varies between -4.7 and -14.6 dBm. Second, over a range of operating microwave power levels the path loss at a particular microwave and doppler frequency is approximately constant. Finally, the BARITT devices show a 1/f noise characteristic for low doppler frequencies. In X-band BARITT devices the corner frequency of this noise could be changed by changing the device diffusion temperature and time. Presumably this may also be the case for the K-band devices.

To compare the operation of BARITT self-oscillating detectors with similar devices, the characteristics of a self-oscillating IMPATT, a self-oscillating Gunn and a Schottky detector pumped with a Gunn oscillator were measured. The IMPATT and Gunn-pumped Schottky results are shown in Figs. 7 and 8, respectively. Even with the IMPATT showing no 1/f characteristic the BARITT device is superior, requiring smaller dc and microwave power and having better path loss and MDS characteristics. The BARITT device is also superior to both the self-oscillating Gunn and the particular Gunn-pumped Schottky tested.

References

1. East, J. R., Nguyen-Ba, H. and Haddad, G. I., "Design, Fabrication, and Evaluation of BARITT Devices for Doppler System Applications," IEEE Trans. on Microwave Theory and Techniques, vol. MTT-24, No. 12, pp. 943-948, December 1976.

2. Gupta, M. S., Lomax, R. J. and Haddad, G. I., "Noise Considerations in Self-Mixing IMPATT Diode Oscillators for Short-Range Doppler Radar Applications," IEEE Trans. on Microwave Theory and Techniques, vol. MTT-22, No. 1, pp. 37-43, January 1974.

3. Nygren, T. and Sjölund, A., "Sensitivity of Doppler Radar and Self Detecting Diode Oscillators," IEEE Trans. on Microwave Theory and Techniques, vol. MTT-22, No. 5, pp. 494-498, May 1974.

4. Mouthaan, K., "Characterization of Nonlinear Interactions in Avalanche Transit-Time Oscillators, Frequency Multipliers, and Frequency Dividers," IEEE Trans. on Microwave Theory and Techniques, vol. MTT-18, No. 11, pp. 853-862, November 1970.

5. Hines, M. E., "Large-Signal Noise, Frequency Conversion, and Parametric Instabilities in IMPATT Diode Networks," Proc. IEEE, vol. 60, No. 12, pp. 1534-1548, December 1972.

6. Fikart, J. L., "AM and FM Noise in BARITT Oscillators," IEEE Trans. on Microwave Theory and Techniques, vol. MTT-22, No. 5, pp. 517-523, May 1974.

Table 1

Parameters for Si p^+np^+ Diodes

Diode	A	B	Experimental
Doping $(cm)^{-3}$	4×10^{15}	4.7×10^{15}	$\approx 4 \times 10^{15}$
Base Width (μm)	3.0	2.7	$\approx$3.0
Diameter	-	-	$\approx$0.002 inch
Specified Load Resistance (Ω-cm^2)	3×10^{-5}	2×10^{-5}	-

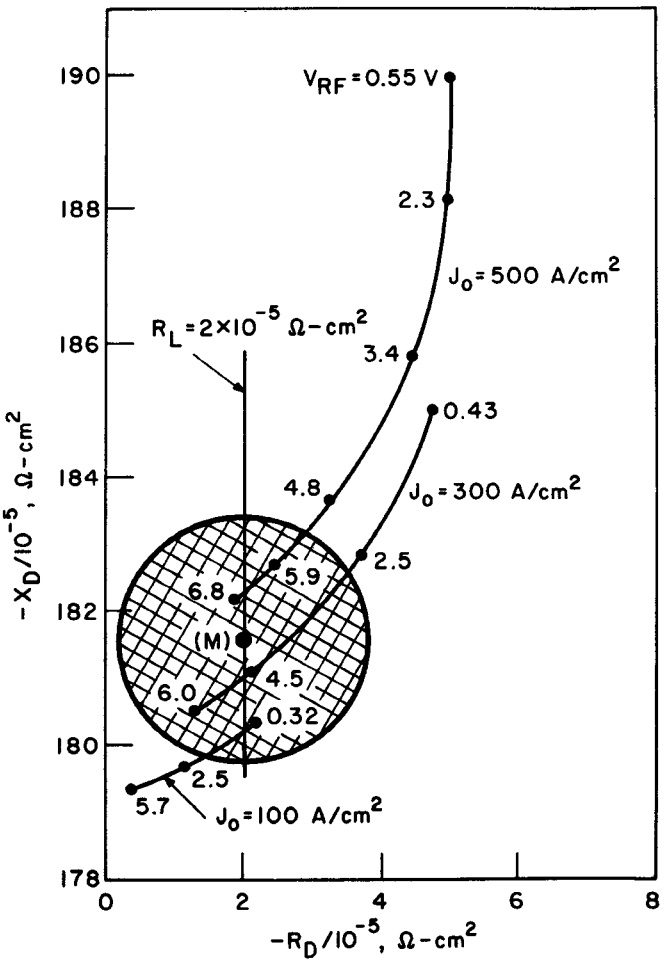

Fig. 1 R-X Plot for Diode B. (f = 23 GHz)

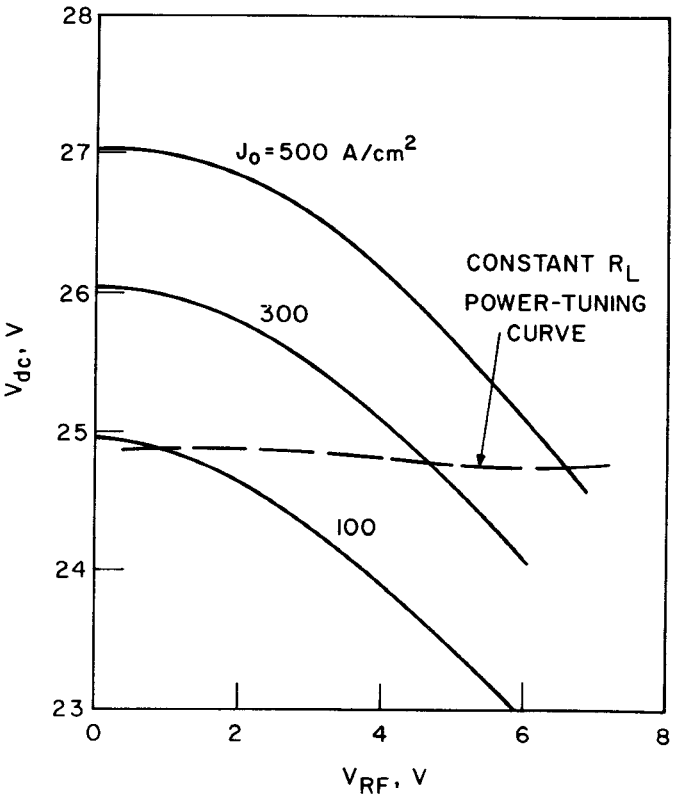

Fig. 2 Rectification Effect Between the Bias Voltage and the RF Drive. (Diode B, f = 23 GHz)

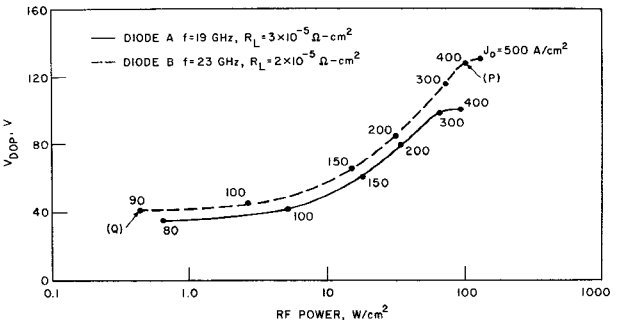

Fig. 3 Normalized Detected Doppler Signal Voltage vs. RF Power.

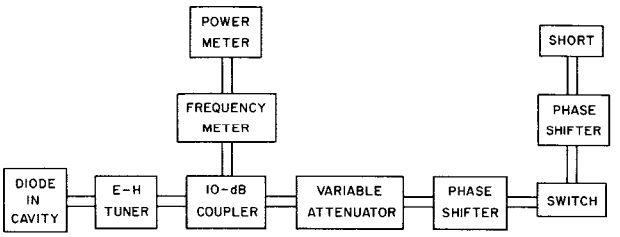

Fig. 4 Microwave Test Circuit for Self-Oscillating Doppler Detectors.

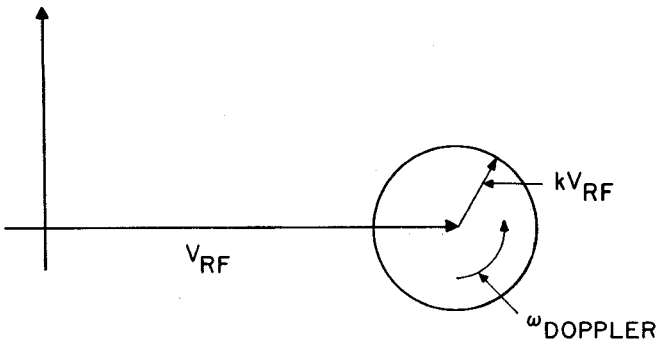

Fig. 5 Phasor Diagram of Doppler Test Circuit.

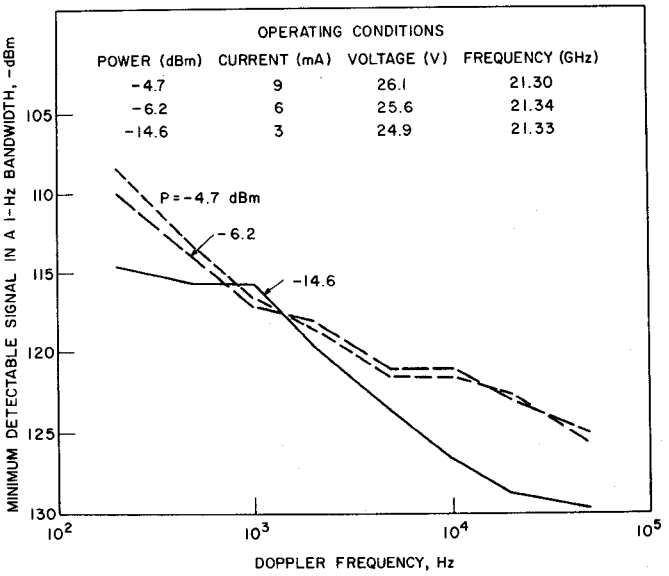

Fig. 6 BARITT Doppler Detector Sensitivity. (21.3 GHz)

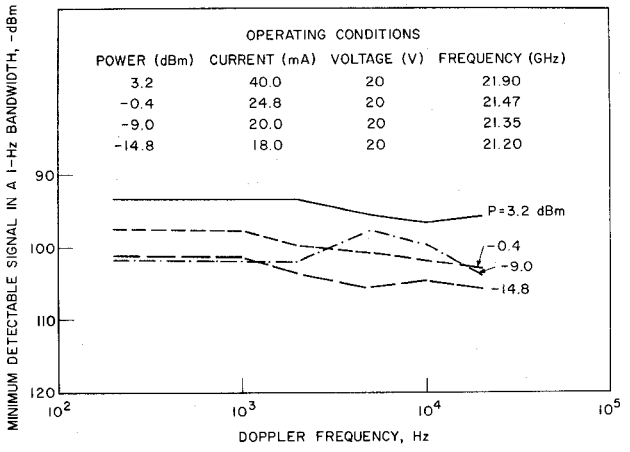

Fig. 7 IMPATT Doppler Detector Sensitivity. (21.9 GHz)

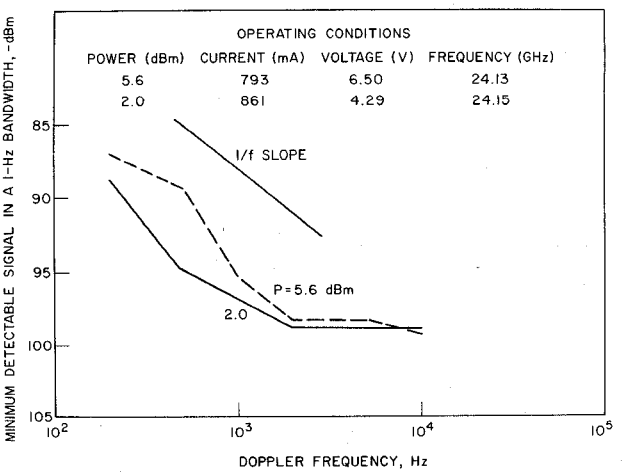

Fig. 8 Gunn Diode Pumped Schottky Detector Module Sensitivity. (24.1 GHz)